Published in final edited form as:
Neurotoxicology. 2013 January ; 34: 160–166. doi:10.1016/j.neuro.2012.10.014.

Manganese inhibits ATP-induced calcium entry through the transient receptor potential channel TRPC3 in astrocytes

Karin Streifel[1], **James Miller**[1], **Rola Mouneimne**[2], and **Ronald B. Tjalkens**[1,*]

[1]Center for Environmental Medicine, Department of Environmental and Radiological Health Sciences, Colorado State University

[2]Department of Veterinary Integrative Biosciences, Texas A&M University

Abstract

Chronic exposure to elevated levels of manganese (Mn^{2+}) causes neuronal injury and inflammatory activation of glia. Astrocytes selectively accumulate Mn^{2+}, which inhibits mitochondrial respiration and increases production of reactive oxygen species. We previously reported that sub-acute exposure to low micromolar levels of Mn^{2+} in primary astrocytes inhibited ATP-induced calcium (Ca^{2+}) signaling, associated with decreased levels of endoplasmic reticulum Ca^{2+} and increased mitochondrial Ca^{2+} loads. In the present studies, we postulated that the mechanism underlying the capacity of Mn^{2+} to inhibit these purinergic signals in astrocytes could be due to competition with Ca^{2+} for entry through a plasma membrane channel. These data demonstrate that acutely applied Mn^{2+} rapidly inhibited ATP-induced Ca^{2+} waves and transients in primary striatal astrocytes. Mn^{2+} also decreased influx of extracellular Ca^{2+} induced by 1-oleoyl-2-acetyl-sn-glycerol (OAG), a direct activator of the transient receptor potential channel, TRPC3. The TRPC3 inhibitor, pyrazole-3, prevented ATP- and OAG-dependent transport of Mn^{2+} from extracellular stores, demonstrated by a dramatic reduction in the rate of fluorescence quenching of Fura-2. These data indicate that Mn^{2+} can acutely inhibit ATP-dependent Ca^{2+} signaling in astrocytes by blocking Ca^{2+} entry through the receptor-operated cation channel, TRPC3. Loss of normal astrocytic responses to purinergic signals due to accumulation of Mn^{2+} could therefore comprise critical homeostatic functions necessary for metabolic and trophic support of neurons.

Keywords

Astrocytes; Calcium; TRP channels; Manganese; ATP

*Corresponding Author Ronald B. Tjalkens, Ph.D. Department of Environmental and Radiological Health Sciences Colorado State University 1680 Campus Delivery Fort Collins, CO 80523-1680 Tel: +1 970 491 2825 Fax: +1 970 491 7569 Ron.Tjalkens@colostate.edu.

Conflict of interest
The authors declare that there are no conflicts of interest.

1. Introduction

Manganese (Mn^{2+}) is essential for normal development and physiological function but high-level exposure leads to a progressive neurodegenerative condition in the basal ganglia, as well as other sub-cortical and cortical structures, that is accompanied by neuroinflammatory activation of glial cells. Manganese is required for a number of critical enzymes in the CNS including Mn-superoxide dismutase and glutamine synthetase, the latter of which is exclusively expressed in astrocytes and accounts for 80% of total brain Mn^{2+} (Norenberg and Martinez-Hernandez, 1979, Wedler and Denman, 1984). Elevated levels of Mn^{2+} accumulate in the basal ganglia, particularly in astrocytes, resulting in phenotypic changes characteristic of inflammatory activation (Hazell, 2002). Astrocytes take up Mn^{2+} through high-affinity transport systems such as the divalent metal transporter 1 (DMT-1) and transferrin receptor (Aschner et al., 1992, Erikson and Aschner, 2006). Additional membrane channels are also implicated in Mn^{2+} transport in astrocytes (Aschner et al., 1992, Crossgrove and Yokel, 2005, Tjalkens et al., 2006, Yokel, 2009), suggesting a complex mechanism for maintaining Mn^{2+} homeostasis that likely relies on multiple specific and general transporters.

Previous studies from our laboratory reported that sub-acute exposure to low micromolar levels of Mn^{2+} in primary cultured astrocytes inhibited ATP-induced calcium (Ca^{2+}) signaling (Tjalkens et al., 2006). The observed inhibition of Ca^{2+} waves and transients was associated with a depletion of thapsigargin-sensitive intracellular stores, implicating inhibition of store-operated channels as possible mechanism in the decreased Ca^{2+} response to ATP. ATP is a major paracrine signaling factor that mediates the transmission of intercellular Ca^{2+} waves between astrocytes that are important for regulation of synaptic function, metabolism, and cerebral blood flow (Haydon and Carmignoto, 2006). Astrocytic responses to ATP are mediated by P_2Y and P_2X purinergic receptors; P_2Y metabotropic receptors are activated by low physiological levels of extracellular ATP (0.1 - 10 μM), whereas P_2X ionotropic receptors are activated at high levels of ATP (>100 μM) that are often associated with neurological injury (James and Butt, 2002). Activation of P_2Y receptors is coupled to phospholipase C (PLC)-mediated generation of inositol triphosphate (IP_3), which causes release of Ca^{2+} from the endoplasmic reticulum, as well as generation of diacylglycerol (DAG), which stimulates Ca^{2+} entry from extracellular stores.

Because DAG is a known activator of the transient receptor potential (TRP) channel TRPC3 (Hofmann et al., 1999), we postulated that this plasma membrane channel could be a site of inhibition of Ca^{2+} influx by Mn^{2+}. It has been reported that TRPC3 in astrocytes mediates Ca^{2+} entry (Grimaldi et al., 2003) and high levels of TRPC3 mRNA are expressed in the basal ganglia in both rodent (Grimaldi et al., 2003, Kunert-Keil et al., 2006) and human (Riccio et al., 2002). Furthermore, studies in vascular smooth muscle cells reported that TRPC3 activation is associated with stimulation of pyrimidine receptors (Reading et al., 2005) and is likely a common pathway in for Ca^{2+} entry via PLC-coupled channels (Hofmann et al., 1999, Lintschinger et al., 2000). Thus, the capacity of Mn^{2+} to inhibit ATP-induced Ca^{2+} signaling in astrocytes could be mediated by competition for Ca^{2+} entry through TRP channels, thereby decreasing the amplitude of evoked Ca^{2+} waves and transients. Mn^{2+} can substitute for Ca^{2+} in a number of transport processes due to similarities in both valence and atomic radius but can also inhibit critical Ca^{2+} transporters (Chance, 1965, Gunter et al., 2006).

In contrast to previous studies using longer exposures to Mn^{2+}, we set out to identify whether acutely administered Mn^{2+} could rapidly block ATP-activated Ca^{2+} signaling in astrocytes by inhibiting Ca^{2+} influx across the plasma membrane. We observed that Mn^{2+} rapidly inhibited mechanically-induced Ca^{2+} waves in astrocytes and similarly decreased the

amplitude of ATP-induced Ca^{2+} transients. Mn^{2+} also decreased Ca^{2+} transients in astrocytes induced by the DAG mimic, 1-oleoyl-2-acetyl-sn-glycerol (OAG), a direct activator of TRPC3. Using the Fura-2 quenching technique, we demonstrated that both ATP and OAG caused entry of extracellular Mn^{2+} into astrocytes that rapidly quenched Fura-2 fluorescence. Mn-dependent quenching of Fura-2 in response to ATP or OAG was prevented by the TRPC3 inhibitor, pyrazole-3 (Pyr3). Collectively, these data suggest that TRPC3 is a receptor-operated plasma membrane channel involved in ATP-induced Ca^{2+} signaling in astrocytes which may be a novel target of Mn^{2+} that broadly decreases the response to purinergic signals.

2. Material and Methods

Mice (*Mus musculus,* C57Bl/6J) were obtained from the Jackson Laboratory (Bar Harbor, ME), cell culture media supplemented with Earle's Salts and L-glutamine was purchase from Hylcone (Logan, UT), Hank's Balanced Salt Solution from GIBCO (Grand Island, NY), and fetal bovine serum and penicillin-streptomycin-neomycin were purchases from Invitrogen (Carlsbad, CA). Fluo-4 AM and Fura-2 dyes were purchased from Molecular Probes (Eugene, OR) and OAG was from Millipore (Bedford, MA). All other chemical reagents were ordered form Sigma Aldrich (St. Louis, MO) unless otherwise stated.

2.1. Cell culture

Primary striatal astrocytes were isolated from 1 - 3 day old C57Bl/6J mice, as previously described (Aschner and Kimelberg, 1991, Moreno et al., 2008). Striatal hemispheres were rapidly dissected, extracted, and maintained in Minimal Essential Media (MEM) supplemented with Earle's Salts and L-glutamine, with 10% Fetal Bovine Serum and 1% penicillin-streptomycin-neomycin (Life Technologies, Carlsbad, CA). Cells were grown to confluence at 37°C, 5% CO_2 in a humid atmosphere for approximately three weeks. Cells were sub-cultured onto 4-well poly-D-lysine-coated cover glass chambered slides (Nalgene-Nunc, Rochester, NY) and allowed to grow to semi-confluence. In our laboratory, cultures consistently yield >98% astrocytes as determined by immunofluorescence staining for glial fibrillary acidic protein (Tjalkens et al., 2006). All procedures involving animals were conducted under a protocol approved by the Animal Care and Use Committee at Colorado State University according to the guidelines of the National Institutes of Health.

2.2. Calcium Imaging

Astrocytes were sub-cultured to approximately 75% confluency on 4-well chamber slides and incubated with 2 μM of Fluo-4 AM (ex: 490 nm, em: 515 nm) for 15 minutes at 37°C prior to imaging. Cells were imaged in media (MEM, without phenol red or sodium bicarbonate) supplemented with 10 mM HEPES buffer (pH 7.4) at 25 °C. The composition of inorganic salts in the media is: 1.8 mM $CaCl_2$, 0.8 mM $MgSO_4$, 5.3 mM KCl, 117 mM NaCl, and 1 mM $NaPO_4$. Groups of approximately 15-30 contiguous cells per field of view were identified for imaging. Cells were stimulated with 1 μM ATP to selectively activate G protein-coupled (GPCR) metabotropic purinergic receptors rather than ionotropic receptors, (James and Butt, 2002) or with 1-oleoyl-2-acetyl-sn-glycerol (OAG; 100 μM), a selective TRPC channel agonist. Mn^{2+} was added 30 seconds prior to each agonist and images of Fluo-4 fluorescence were collected every 500 milliseconds for 120 seconds with camera binning set at 4×4 pixels with an exposure time of approximately 20 milliseconds. To observe recovery of Ca^{2+} transients three additions of 1 μM ATP we applied and washed out with imaging media after each application using a continuous flow cell. Prior to the second ATP addition Mn^{2+} (10 μM) was added to the imaging media for 30 seconds. Images were collected on a Zeiss Axiovert 200M microscope equipped with a Hammatsu ORCA-ER cooled charge-coupled device camera. Fluorescent intensity was expressed

relative to the baseline image (F/F_0), where F_0 is the fluorescence level prior to stimulation. Datasets were analyzed using Slidebook software (v5.0; Intelligent Imaging Innovations, Inc., Denver, CO).

2.3. Mechanically-induced calcium waves

For Ca^{2+} wave propagation studies, astrocytes were sub-cultured onto poly-D-lysine coated 30 mm round glass coverslips and placed in a flow chamber (POCmini, Carl Zeiss, New York, NY). After collection of baseline Fluo-4 intracellular Ca^{2+} intensity for 10 seconds, Ca^{2+} waves were mechanically-induced with a 5 μm diameter drawn glass micropipet using a micromanipulator. Mn^{2+} was added approximately 30 seconds prior to stimulation and images were acquired every 500 milliseconds for 60 seconds. Fluorescent intensity was expressed relative to the baseline image (F/F_0) in all cells within the wave activation site. Wave amplitude and distance were determined using Slidebook software (v5.0; Intelligent Imaging Innovations, Inc., Denver, CO).

2.4. Fura-2 quenching

Studies examining fluorescence quenching of the dye Fura-2 by Mn^{2+} were performed as previously described (Grimaldi, 2006), with slight modifications. Primary astrocytes subcultured into 4-well chambered slides were loaded for 25 minutes at 25 °C with 4 μM Fura-2 AM in Ca^{2+} containing HEPES-buffered Hank's Balanced Salt Solution (HBSS; Life Technologies, Carlsbad, CA). Cells were then rinsed with fresh buffer and incubated for an additional 25 minutes with either the TRPC3 specific inhibitor, Pyr3 (10 μM) or DMSO (0.1%) in Ca^{2+} containing HEPES-buffered HBSS at 37 °C. Prior to Fura-2 imaging the cells were rinsed with Ca^{2+}-free HEPES-buffered HBSS. Images of Fura-2 fluorescence were collected every second for 15 minutes at ex: 340 nm, em: 510 nm, in order to detect quenching of the Fura-2 signal. Baseline fluorescence was established for the first 60 seconds and the cells were then stimulated with either 1 μM ATP or 100 μM OAG for an additional 6 minutes followed by 100 μM Mn^{2+} for the remaining 8 minutes. Fluorescence intensity was expressed relative to baseline (F/F_0).

2.5. Statistical analysis

Comparisons three or more means with one independent variable was performed using one-way analysis of variance (ANOVA) followed by the Tukey's multiple *post hoc* test using Prism software (v4.0c, Graphpad Software, Inc., San Diego, CA). Comparison of two-group comparisons were analyzed using the Student's t-test. The rate of Fura-2 quenching was determined through non-linear regression. Results are expressed as the mean ± SEM from a minimum of 3 independent studies and for all experiments, $p<0.05$ was considered significant.

3. Results

3.1. Acute Mn^{2+} exposure decreases physiological glial-glial communication in striatal astrocytes

To examine the effect of Mn^{2+} on intercellular Ca^{2+} wave propagation in astrocytes, we mechanically stimulated a single cell in the center of a confluent field with a 0.5 μm glass micropipet to initiate ATP-dependent Ca^{2+} waves (Newman, 2001). The response was recorded using the Ca^{2+}-sensitive dye, Fluo-4 AM, which does not significantly interact with Mn^{2+} (Bird et al., 2008, Johnson, 2010). Mechanical stimulation of control cells elicited robust intercellular Ca^{2+} waves that diminished in intensity approximately 500 μm away from the site of activation (Figure 1 a,b). Following the acute application of 10 μM Mn^{2+} to the extracellular media, the maximum amplitude of the intercellular Ca^{2+} transients

from mechanically-induced intercellular waves was significantly decreased (Figure 1 c,d). Kymograph images of the Ca^{2+} wavefront indicated that acute exposure to Mn^{2+} decreased the intensity of the wave uniformly throughout the astrocyte syncytium (Figure 1 b,d). Similarly, the average intensity and distance of propagation of Ca^{2+} waves was decreased following acute application of Mn^{2+} to the imaging medium (Figure 1 e-h).

3.2. Acute application of Mn^{2+} decreases ATP-induced Ca^{2+} transients

Activation of metabotropic purinergic receptors with physiological levels of ATP resulted in rapid increases in intracellular Ca^{2+} that were inhibited by acute application of Mn^{2+} (Figure 2 a,b). The shape of the ATP-induced transient reflects biphasic Ca^{2+} release, first from intracellular stores of the endoplasmic reticulum followed by an influx of Ca^{2+} from the extracellular space driven by the electrochemical gradient of Ca^{2+} through activation of channels in the plasma membrane. However, when Mn^{2+} was acutely added to the extracellular medium, the Ca^{2+} response was dose-dependently inhibited by low levels of Mn^{2+}, with maximal inhibition observed as low as 10 μM Mn^{2+} (Figure 2 c,d). The concentration of Mn^{2+} added was only slightly above physiologic levels in the CNS, which are normally 2-8 μM (Pal et al., 1999). Representative traces and quantitative analysis of the average amplitude revealed a very steep dose-response curve that indicates a low threshold concentration at which Mn^{2+} acutely inhibits purinergic Ca^{2+} signaling in striatal astrocytes (Figure 2 c,d). Using a flow-cell chamber to examine the reversibility of the acute Mn^{2+} effect on ATP-induced Ca^{2+} transients (Figure 2 e,f), we found that control cells responded to ATP with repeated elevations in intracellular Ca^{2+} that were reversibly inhibited by Mn^{2+} at concentrations as low as 10 μM.

3.3. Mn^{2+} interferes with OAG-induced Ca^{2+} entry through plasma membrane channels in striatal astrocytes

We postulated that the acute inhibitory effect of Mn^{2+} could be due to interference with Ca^{2+} influx into the astrocyte from extracellular stores. The non-selective cation channel TRPC3 is found in high abundance in the mid-brain and striatum of mice (Kunert-Keil et al., 2006) and could therefore could be a target for Mn^{2+} in astrocytes. The TRPC agonist, OAG, is an analog of DAG that selectively activates TRPC3, TRPC6 and TRPC7 receptors (Hofmann et al., 1999). Application of 100 μM OAG caused a robust Ca^{2+} response in astrocytes (Figure 3 a,b) that was attenuated in the presence of Mn^{2+} (Figure 3 b,c). The TRPC3 antagonist pyrazole-3 (Pyr3)(Kiyonaka et al., 2009) also suppressed ATP-induced Ca^{2+} transients, similarly to Mn^{2+} (Figure 3 e,f), strongly implicating the involvement of this channel in Ca^{2+} entry from extracellular stores as a result of ATP-induced transients in striatal astrocytes.

3.4. Mn^{2+} influx occurs through TRPC3 in striatal astrocytes

To examine the site of Mn^{2+} inhibition of OAG-induced Ca^{2+} influx across the plasma membrane in astrocytes, we utilized the ability of Mn^{2+} to quench the fluorescence signal of the Ca^{2+} indicator Fura-2 (Figure 4). Stimulation of astrocytes with 1 μM ATP caused a robust increase in intracellular Ca^{2+} followed by a secondary plateau phase of extracellular Ca^{2+} entry through receptor operated channels. Addition of 100 μM Mn^{2+} after stimulation with ATP resulted in rapid quenching of the Fura-2 fluorescence signal (Figure 4 a,b), plotted as the first order rate of decay (k, $F/F_0 \bullet sec^{-1}$), indicating Mn^{2+} entry into the cell. Likewise, application of Mn^{2+} after OAG caused rapid quenching of Fura-2 fluorescence (Figure 4 c,d). Selective inhibition of TRPC3 by Pyr3 significantly reduced the rate of Mn^{2+} mediated Fura-2 quenching following ATP- or OAG-activated Ca^{2+} entry by 55% and 95%, respectively (Figure 4 b,d).

4. Discussion

Studies examining the effects of Mn^{2+} on astrocyte function have largely focused on outcomes such as inhibition of mitochondrial respiration, loss of ATP, and production of reactive oxygen species (Brouillet et al., 1993, Zwingmann et al., 2003, Gunter et al., 2006). There is far less information on the ability of Mn^{2+} to disrupt Ca^{2+} signaling in astrocytes, although studies in brain mitochondria indicate that Mn^{2+} uptake by the outer mitochondrial membrane Ca^{2+} uniporter causes sustained increases in matrix Ca^{2+} and oxidative stress (Gavin et al., 1990). However, the identity of plasma membrane Ca^{2+} channels that could be targeted by Mn^{2+} is less clear. There are diverse transport mechanisms for Mn^{2+} across the plasma membrane (Aschner et al., 2005) and the present data suggest that one of these Ca^{2+} transporters could be competitively targeted by Mn^{2+}. Our findings demonstrate that Mn^{2+} inhibits Ca^{2+} influx through receptor-activated cation channels in striatal astrocytes. We found that Ca^{2+} waves and transients stimulated by ATP-dependent purinergic signals are acutely inhibited by Mn^{2+}, likely through competition for Ca^{2+} influx through TRPC3 channels. Dampening normal Ca^{2+} responses to purinergic stimuli in astrocytes could have dramatic consequences on neuronal function and survival, because these signaling events are critical for regulation of cerebral energy metabolism, blood flow, and synaptic function (Haydon, 2001), as well as for particular protection against excitotoxic neuronal injury (Pascual et al., 2005). Dysfunction in purinergic Ca^{2+} signaling has been associated with neuroinflammatory and neurodegenerative conditions such as Parkinson's and Alzheimer's disease (Iadecola, 2004, Burnstock et al., 2011) and the non-selective cation channel TRPC3 has been directly associated with pathophysiological activation of astrocytes in response to neuroinflammatory stimuli (Shirakawa, 2012). Thus, inhibition of ATP-dependent Ca^{2+} signaling by excessive exposure to Mn^{2+} could explain some of the phenotypic changes in astrocytes that lead to neuronal injury in brain regions where Mn^{2+} accumulates, such as the basal ganglia.

Propagation of Ca^{2+} waves in confluent astrocyte cultures models the pattern of intercellular Ca^{2+} waves in astrocytes *in situ* (Haydon and Carmignoto, 2006, Ullah et al., 2006). The primary gliotransmitter in astrocytes regulating intercellular Ca^{2+} waves is ATP, released through exocytosis via SNARE proteins (Newman, 2001, James and Butt, 2002, Pascual et al., 2005) and through connexin 43 hemichannels (Kang et al., 2008). Sub-acute exposure to low micromolar concentrations of Mn^{2+} are sufficient to inhibit Ca^{2+} wave activity (Tjalkens et al., 2006), consistent with the capacity of Mn^{2+} to cause mitochondrial sequestration of Ca^{2+} and decreases in thapsigargin-sensitive endoplasmic reticulum Ca^{2+} stores. Data from the present studies (Figure 1) indicated that Mn^{2+} applied only 30 seconds prior to stimulation of astrocytes inhibited both the intensity as well as the total distance travelled of mechanically-induced Ca^{2+} waves. Although these decreases in Ca^{2+} wave activity could result from both direct inhibition of Ca^{2+} channels as well as interference with intracellular second messenger signals (Barhoumi et al., 2010), the ability of similar divalent cations, such as Mg^{2+} and Ni^{2+}, to inhibit Ca^{2+} influx across the plasma membrane (Crossgrove and Yokel, 2004, Ko et al., 2004, Lee et al., 2011) makes it much more likely that the rapid inhibition of Ca^{2+} waves observed with Mn^{2+} is mediated by direct blockade of plasma membrane Ca^{2+} channels in astrocytes.

Acute application of 10 μM Mn^{2+} or greater attenuated ATP-induced Ca^{2+} transients in cultured astrocytes (Figure 2). This concentration of Mn^{2+} is only slightly above that in extracellular fluid in the CNS (Pal et al., 1999) and similar to levels measured in rodent brain in chronic models of Mn^{2+} neurotoxicity (Liu et al., 2006, Aschner et al., 2009, Moreno et al., 2009), suggesting that quite low levels of exogenous Mn^{2+} in the CNS may subtly perturb normal homeostatic functions in astrocytes. However, intracellular Mn^{2+} levels in astrocytes are likely greater, given the high capacity for Mn^{2+} uptake (Erikson and

Aschner, 2006). The reversibility of the effect of Mn^{2+} on ATP-induced transients (Figure 2e) strongly supports the conclusion that plasma membrane Ca^{2+} channels in astrocytes are an acute target of Mn^{2+}. Moreover, extracellular Ca^{2+} is both a competitive and noncompetitive inhibitor of Mn^{2+} uptake for common non-selective sites of entry (Gavin et al., 1990, Crossgrove and Yokel, 2004), likely due to its similar size, oxidation state, and electrochemical properties. Studies in microvasular endothelial cells reported that Ca^{2+} concentrations negatively correlated with Mn^{2+} influx and that Mn^{2+} influx in Ca^{2+}-free media was significantly greater than with Ca^{2+} present (Yokel et al., 2003), suggesting competition for entry through a common channel. Mn^{2+} uptake is also inhibited by the divalent cation Ni^{2+}, which has been shown to inhibit receptor-operated and store-operated channels (Cui and Dannies, 1992, Kukkonen et al., 2001). Collectively, these data indicate that extracellular Mn^{2+} can acutely and reversibly inhibit Ca^{2+} influx in astrocytes.

Although astrocytes express both voltage-gated and receptor-operated Ca^{2+} channels (Barhoumi et al., 2010), we suspected that inhibition of non-selective cation channels permeable to both Ca^{2+} and Mn^{2+} could be responsible for the loss of ATP-induced Ca^{2+} signaling in astrocytes acutely exposed to Mn^{2+}. Concentrations of ATP up to 10 μM activate P_2Y receptors, which are metabotropic G protein-coupled receptors (GPCR) that cause rapid release of Ca^{2+} from intracellular stores through the PLC-IP_3 pathway, with concomitant generation of DAG (James and Butt, 2002). Using the membrane-permeable analog of DAG, OAG, we determined that acutely applied Mn^{2+} inhibited OAG-induced Ca^{2+} transients in astrocytes (Figure 3). OAG activates TRPC3 channels leading to the influx of cations such as Ca^{2+} into astrocytes (Hofmann et al., 1999) and TRPC3 activation results in influx of both Ca^{2+} and Mn^{2+} across the plasma membrane of medullary kidney cells (Goel and Schilling, 2010). The data in Figure 3 (e,f) indicate that the TRPC3 inhibitor, Pyr3, abolished ATP-induced Ca^{2+} transients in striatal astrocytes, similar to Mn^{2+}. Likewise, the rate of Mn^{2+}-dependent quenching of Fura-2 fluorescence was significantly reduced by Pyr3 (Figure 4), strongly implicating TRPC3 as a site of Mn^{2+} influx in astrocytes mediating the observed reduction of Ca^{2+} signals during acute Mn^{2+} exposure. TRPC3 is selectively activated by DAG following stimulation of GPCR receptors, demonstrated by studies in which applied histamine caused rapid influx of Ca^{2+} that was quenched by Mn^{2+}, further demonstrating competition for Ca^{2+} entry at this channel (Hofmann et al., 1999). These studies also reported that TRPC3, but not TRPC4, 5 or 6, was selectively inhibited by Mn^{2+} at concentrations similar to those used here, indicating that inhibition of TRPC channels by Mn^{2+} is highly selective for TRPC3. Of the canonical TRPC family members, it was previously reported that TRPC3 is expressed at significant levels in astrocytes (Grimaldi et al., 2003) and is activated by GPCR activation through the PLC-DAG pathway (Hofmann et al., 1999, Reading et al., 2005). Thus, the capacity of Pyr3 to decrease the rate of Mn-dependent Fura-2 strongly suggests that Mn^{2+} is competing with Ca^{2+} for entry through TRPC3 in response to ATP and OAG.

In conclusion, these studies support the hypothesis that Mn^{2+} acutely inhibits both mechanically stimulated Ca^{2+} waves and ATP-induced Ca^{2+} transients in astrocytes, in part, by preventing influx of extracellular Ca^{2+} through the transient receptor potential channel, TRPC3. The reversibility of this effect also suggests that the basis for this inhibition may be competition with Ca^{2+} for entry via this non-selective cation channel, although more detailed electrophysiological studies are required to determine the precise mechanism. These data indicate that in addition to inhibiting mitochondrial Ca^{2+} signaling (Gavin et al., 1990) and decreasing releasable pools of endoplasmic reticulum Ca^{2+} in astrocytes (Tjalkens et al., 2006), Mn^{2+} can acutely interfere with receptor-operated plasma membrane channels such as TRPC3 and thereby alter the pattern and amplitude of Ca^{2+} signals in response to purinergic signals. Such changes in these fundamental Ca^{2+} signaling pathways in astrocytes

could have negative effects on neuronal function and provide additional insight into the mechanisms underlying the neurotoxicity of excess Mn^{2+}.

Acknowledgments

This work was supported by a grant from the National Institutes of Health (ES012941). We are grateful to Dr. Scott Earley for advice regarding inhibitors of TRPC3.

References

Aschner M, Erikson KM, Dorman DC. Manganese dosimetry: species differences and implications for neurotoxicity. Crit Rev Toxicol. 2005; 35:1–32. [PubMed: 15742901]

Aschner M, Erikson KM, Herrero Hernandez E, Tjalkens R. Manganese and its role in Parkinson's disease: from transport to neuropathology. Neuromolecular Med. 2009; 11:252–266. [PubMed: 19657747]

Aschner M, Gannon M, Kimelberg HK. Manganese uptake and efflux in cultured rat astrocytes. J Neurochem. 1992; 58:730–735. [PubMed: 1729413]

Aschner M, Kimelberg HK. The use of astrocytes in culture as model systems for evaluating neurotoxic-induced-injury. Neurotoxicology. 1991; 12:505–517. [PubMed: 1684034]

Barhoumi R, Qian Y, Burghardt RC, Tiffany-Castiglioni E. Image analysis of Ca2+ signals as a basis for neurotoxicity assays: promises and challenges. Neurotoxicol Teratol. 2010; 32:16–24. [PubMed: 19555758]

Bird GS, DeHaven WI, Smyth JT, Putney JW Jr. Methods for studying store-operated calcium entry. Methods. 2008; 46:204–212. [PubMed: 18929662]

Brouillet EP, Shinobu L, McGarvey U, Hochberg F, Beal MF. Manganese injection into the rat striatum produces excitotoxic lesions by impairing energy metabolism. Exp Neurol. 1993; 120:89–94. [PubMed: 8477830]

Burnstock G, Krugel U, Abbracchio MP, Illes P. Purinergic signalling: from normal behaviour to pathological brain function. Prog Neurobiol. 2011; 95:229–274. [PubMed: 21907261]

Chance B. The Energy-Linked Reaction Of Calcium With Mitochondria. J Biol Chem. 1965; 240:2729–2748. [PubMed: 14304892]

Crossgrove JS, Yokel RA. Manganese distribution across the blood-brain barrier III. The divalent metal transporter-1 is not the major mechanism mediating brain manganese uptake. Neurotoxicology. 2004; 25:451–460. [PubMed: 15019308]

Crossgrove JS, Yokel RA. Manganese distribution across the blood-brain barrier. IV. Evidence for brain influx through store-operated calcium channels. Neurotoxicology. 2005; 26:297–307. [PubMed: 15935202]

Cui ZJ, Dannies PS. Thyrotropin-releasing hormone-mediated Mn2+ entry in perifused rat anterior pituitary cells. Biochem J. 1992; 283(Pt 2):507–513. [PubMed: 1575695]

Erikson KM, Aschner M. Increased manganese uptake by primary astrocyte cultures with altered iron status is mediated primarily by divalent metal transporter. Neurotoxicology. 2006; 27:125–130. [PubMed: 16140386]

Gavin CE, Gunter KK, Gunter TE. Manganese and calcium efflux kinetics in brain mitochondria. Relevance to manganese toxicity. Biochem J. 1990; 266:329–334. [PubMed: 2317189]

Goel M, Schilling WP. Role of TRPC3 channels in ATP-induced Ca2+ signaling in principal cells of the inner medullary collecting duct. Am J Physiol Renal Physiol. 2010; 299:F225–233. [PubMed: 20410214]

Grimaldi M. Astrocytes refill intracellular Ca2+ stores in the absence of cytoplasmic [Ca2+] elevation: a functional rather than a structural ability. J Neurosci Res. 2006; 84:1738–1749. [PubMed: 17016852]

Grimaldi M, Maratos M, Verma A. Transient receptor potential channel activation causes a novel form of [Ca 2+]I oscillations and is not involved in capacitative Ca 2+ entry in glial cells. J Neurosci. 2003; 23:4737–4745. [PubMed: 12805313]

Gunter TE, Gavin CE, Aschner M, Gunter KK. Speciation of manganese in cells and mitochondria: a search for the proximal cause of manganese neurotoxicity. Neurotoxicology. 2006; 27:765–776. [PubMed: 16765446]

Haydon PG. GLIA: listening and talking to the synapse. Nat Rev Neurosci. 2001; 2:185–193. [PubMed: 11256079]

Haydon PG, Carmignoto G. Astrocyte control of synaptic transmission and neurovascular coupling. Physiol Rev. 2006; 86:1009–1031. [PubMed: 16816144]

Hazell AS. Astrocytes and manganese neurotoxicity. Neurochem Int. 2002; 41:271–277. [PubMed: 12106778]

Hofmann T, Obukhov AG, Schaefer M, Harteneck C, Gudermann T, Schultz G. Direct activation of human TRPC6 and TRPC3 channels by diacylglycerol. Nature. 1999; 397:259–263. [PubMed: 9930701]

Iadecola C. Neurovascular regulation in the normal brain and in Alzheimer's disease. Nat Rev Neurosci. 2004; 5:347–360. [PubMed: 15100718]

James G, Butt AM. P2Y and P2X purinoceptor mediated Ca2+ signalling in glial cell pathology in the central nervous system. Eur J Pharmacol. 2002; 447:247–260. [PubMed: 12151016]

Johnson IaTZS, Michelle, editor. The Molecular Probes Handbook. Life Technologies Corporation; 2010.

Kang J, Kang N, Lovatt D, Torres A, Zhao Z, Lin J, Nedergaard M. Connexin 43 hemichannels are permeable to ATP. J Neurosci. 2008; 28:4702–4711. [PubMed: 18448647]

Kiyonaka S, Kato K, Nishida M, Mio K, Numaga T, Sawaguchi Y, Yoshida T, Wakamori M, Mori E, Numata T, Ishii M, Takemoto H, Ojida A, Watanabe K, Uemura A, Kurose H, Morii T, Kobayashi T, Sato Y, Sato C, Hamachi I, Mori Y. Selective and direct inhibition of TRPC3 channels underlies biological activities of a pyrazole compound. Proc Natl Acad Sci U S A. 2009; 106:5400–5405. [PubMed: 19289841]

Ko EA, Park WS, Earm YE. Extracellular Mg(2+) blocks endothelin-1-induced contraction through the inhibition of non-selective cation channels in coronary smooth muscle. Pflugers Arch. 2004; 449:195–204. [PubMed: 15258766]

Kukkonen JP, Lund PE, Akerman KE. 2-aminoethoxydiphenyl borate reveals heterogeneity in receptor-activated Ca(2+) discharge and store-operated Ca(2+) influx. Cell Calcium. 2001; 30:117–129. [PubMed: 11440469]

Kunert-Keil C, Bisping F, Kruger J, Brinkmeier H. Tissue-specific expression of TRP channel genes in the mouse and its variation in three different mouse strains. BMC Genomics. 2006; 7:159. [PubMed: 16787531]

Lee M, Jantaratnotai N, McGeer E, McLarnon JG, McGeer PL. Mg2+ ions reduce microglial and THP-1 cell neurotoxicity by inhibiting Ca2+ entry through purinergic channels. Brain Res. 2011; 1369:21–35. [PubMed: 21040713]

Lintschinger B, Balzer-Geldsetzer M, Baskaran T, Graier WF, Romanin C, Zhu MX, Groschner K. Coassembly of Trp1 and Trp3 proteins generates diacylglycerol- and Ca2+-sensitive cation channels. J Biol Chem. 2000; 275:27799–27805. [PubMed: 10882720]

Liu X, Sullivan KA, Madl JE, Legare M, Tjalkens RB. Manganese-induced neurotoxicity: the role of astroglial-derived nitric oxide in striatal interneuron degeneration. Toxicol Sci. 2006; 91:521–531. [PubMed: 16551646]

Moreno JA, Sullivan KA, Carbone DL, Hanneman WH, Tjalkens RB. Manganese potentiates nuclear factor-kappaB-dependent expression of nitric oxide synthase 2 in astrocytes by activating soluble guanylate cyclase and extracellular responsive kinase signaling pathways. J Neurosci Res. 2008; 86:2028–2038. [PubMed: 18335517]

Moreno JA, Yeomans EC, Streifel KM, Brattin BL, Taylor RJ, Tjalkens RB. Age-dependent susceptibility to manganese-induced neurological dysfunction. Toxicol Sci. 2009; 112:394–404. [PubMed: 19812362]

Newman EA. Propagation of intercellular calcium waves in retinal astrocytes and Muller cells. J Neurosci. 2001; 21:2215–2223. [PubMed: 11264297]

Norenberg MD, Martinez-Hernandez A. Fine structural localization of glutamine synthetase in astrocytes of rat brain. Brain Res. 1979; 161:303–310. [PubMed: 31966]

Pal PK, Samii A, Calne DB. Manganese neurotoxicity: a review of clinical features, imaging and pathology. Neurotoxicology. 1999; 20:227–238. [PubMed: 10385886]

Pascual O, Casper KB, Kubera C, Zhang J, Revilla-Sanchez R, Sul JY, Takano H, Moss SJ, McCarthy K, Haydon PG. Astrocytic purinergic signaling coordinates synaptic networks. Science. 2005; 310:113–116. [PubMed: 16210541]

Reading SA, Earley S, Waldron BJ, Welsh DG, Brayden JE. TRPC3 mediates pyrimidine receptor-induced depolarization of cerebral arteries. Am J Physiol Heart Circ Physiol. 2005; 288:H2055–2061. [PubMed: 15604128]

Riccio A, Medhurst AD, Mattei C, Kelsell RE, Calver AR, Randall AD, Benham CD, Pangalos MN. mRNA distribution analysis of human TRPC family in CNS and peripheral tissues. Brain Res Mol Brain Res. 2002; 109:95–104. [PubMed: 12531519]

Shirakawa H. Pathophysiological Significance of Canonical Transient Receptor Potential (TRPC) Subfamily in Astrocyte Activation. Yakugaku Zasshi. 2012; 132:587–593. [PubMed: 22687694]

Tjalkens RB, Zoran MJ, Mohl B, Barhoumi R. Manganese suppresses ATP-dependent intercellular calcium waves in astrocyte networks through alteration of mitochondrial and endoplasmic reticulum calcium dynamics. Brain Res. 2006; 1113:210–219. [PubMed: 16934782]

Ullah G, Jung P, Cornell-Bell AH. Anti-phase calcium oscillations in astrocytes via inositol (1, 4, 5)-trisphosphate regeneration. Cell Calcium. 2006; 39:197–208. [PubMed: 16330095]

Wedler FC, Denman RB. Glutamine synthetase: the major Mn(II) enzyme in mammalian brain. Curr Top Cell Regul. 1984; 24:153–169. [PubMed: 6149889]

Yokel RA. Manganese flux across the blood-brain barrier. Neuromolecular Med. 2009; 11:297–310. [PubMed: 19902387]

Yokel RA, Crossgrove JS, Bukaveckas BL. Manganese distribution across the blood-brain barrier. II. Manganese efflux from the brain does not appear to be carrier mediated. Neurotoxicology. 2003; 24:15–22. [PubMed: 12564378]

Zwingmann C, Leibfritz D, Hazell AS. Energy metabolism in astrocytes and neurons treated with manganese: relation among cell-specific energy failure, glucose metabolism, and intercellular trafficking using multinuclear NMR-spectroscopic analysis. J Cereb Blood Flow Metab. 2003; 23:756–771. [PubMed: 12796724]

Highlights (Streifel et al.)

- Manganese rapidly inhibits calcium waves in astrocytes
- ATP- and OAG-induced calcium transients are suppressed by manganese
- The TRPC3 inhibitor pyrazole-3 prevents manganese entry in astrocytes

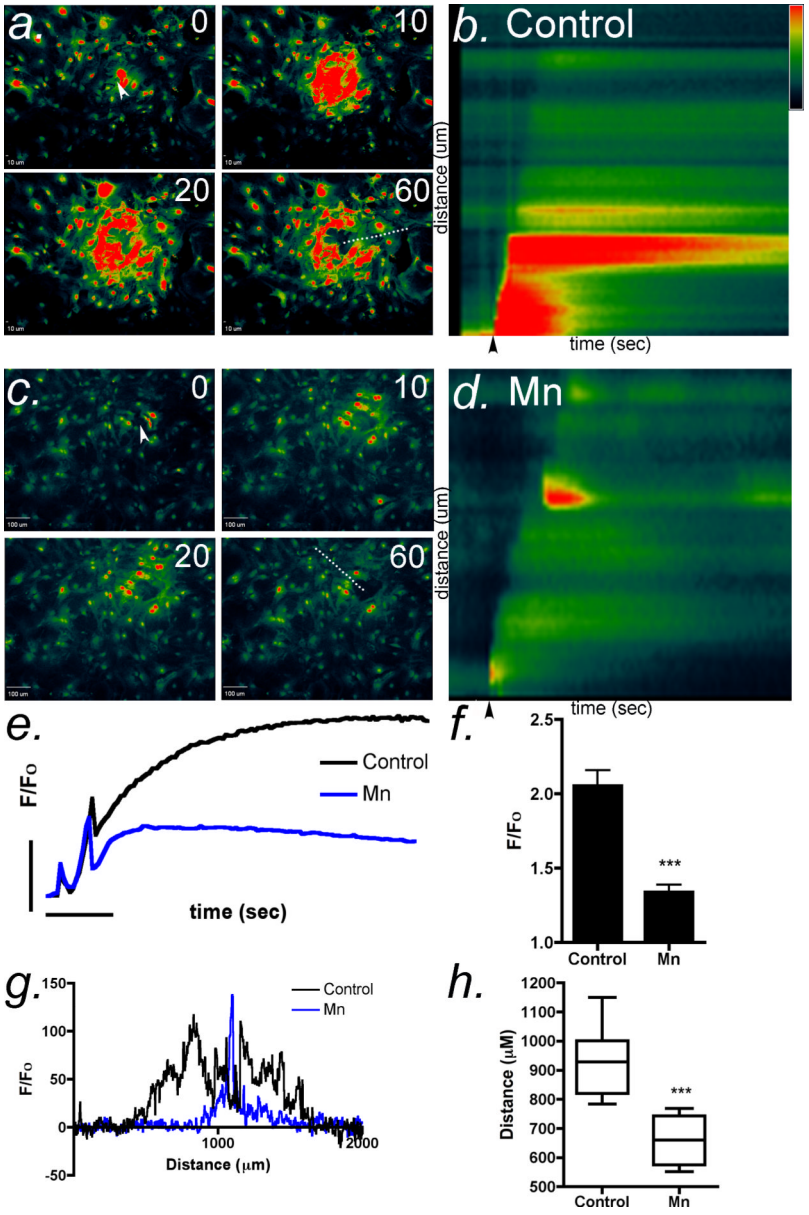

Figure 1. Manganese acutely inhibits calcium wave propagation in striatal astrocytes

(a) Calcium waves were initiated in confluent cultures of striatal astrocytes loaded with Fluo-4 AM (2 μM) using a glass micropipette to stimulate a single astrocyte in the center of the field (white arrow). Images were collected every 500 msec for 60 sec. (b) Kymograph images were generated from the fluorescence intensity of Fluo-4 along a representative line drawn from the point of stimulation to the terminus of the Ca^{2+} wave across across the field of astrocytes (a, dotted line). Black arrows denote the point of stimulation. (c,d) The extent and intensity of Ca^{2+} waves is sharply diminished by acute application of Mn^{2+}. (e,f) The mean intensity of intracellular Ca^{2+} responses in the cells acutely exposed to Mn^{2+} is significantly decreased compared to control. The vertical bar in (e) denotes 1 relative fluorescent unit; the horizontal bar denotes 10 sec. (g) Representative traces of the total distance of the wave front in control and Mn-treated cells. (h) Quantitative analysis of Ca^{2+} wave propagation indicates that Mn^{2+} decreases the distance traveled in striatal astrocytes

by >70% relative to control (n=3 waves analyzed per group for each experiment over 3-4 independent experiments in separate cultures of striatal astrocytes; *** p<0.001).

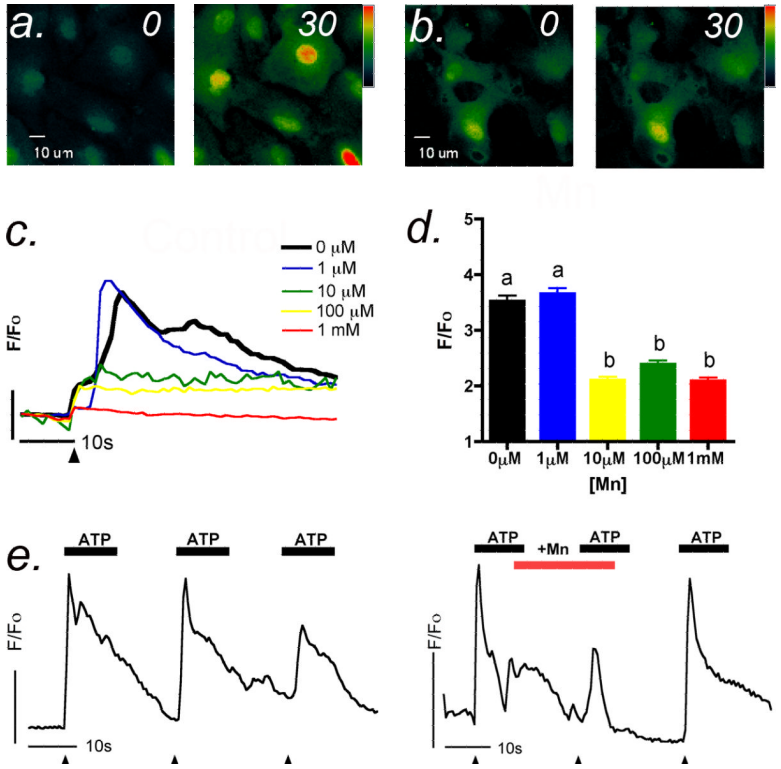

Figure 2. ATP-induced calcium transients are reversibly inhibited by low concentrations of manganese

(a) Application of 1 μM ATP resulted in robust Ca^{2+} transients in striatal astrocytes that persisted for greater than 30 sec. (b) Addition of Mn^{2+} to the imaging media at concentrations as low as 10 μM acutely suppressed ATP-induced Ca^{2+} transients. (c) Representative traces of the astrocytic response to 1 μM ATP (black arrowhead indicates time of ATP addition) in the presence of increasing concentrations of Mn^{2+} (1 - 1000 μM) indicate a dose-dependent suppression of intracellular Ca^{2+} transients. (d) Quantitation of the maximum astrocytic Ca^{2+} response to 1 μM ATP in the presence of increasing concentrations of Mn^{2+}. (e) Repeated additions of 1 μM ATP to striatal astrocytes using a flow chamber induce multiple Ca^{2+} transients that are reversibly inhibited by acute addition (f) of 10 μM Mn^{2+} to the flow cell. Vertical bars denote 1 relative fluorescent unit; horizontal bars denote 10 sec (n= 50-60 cells group; *** p<0.001).

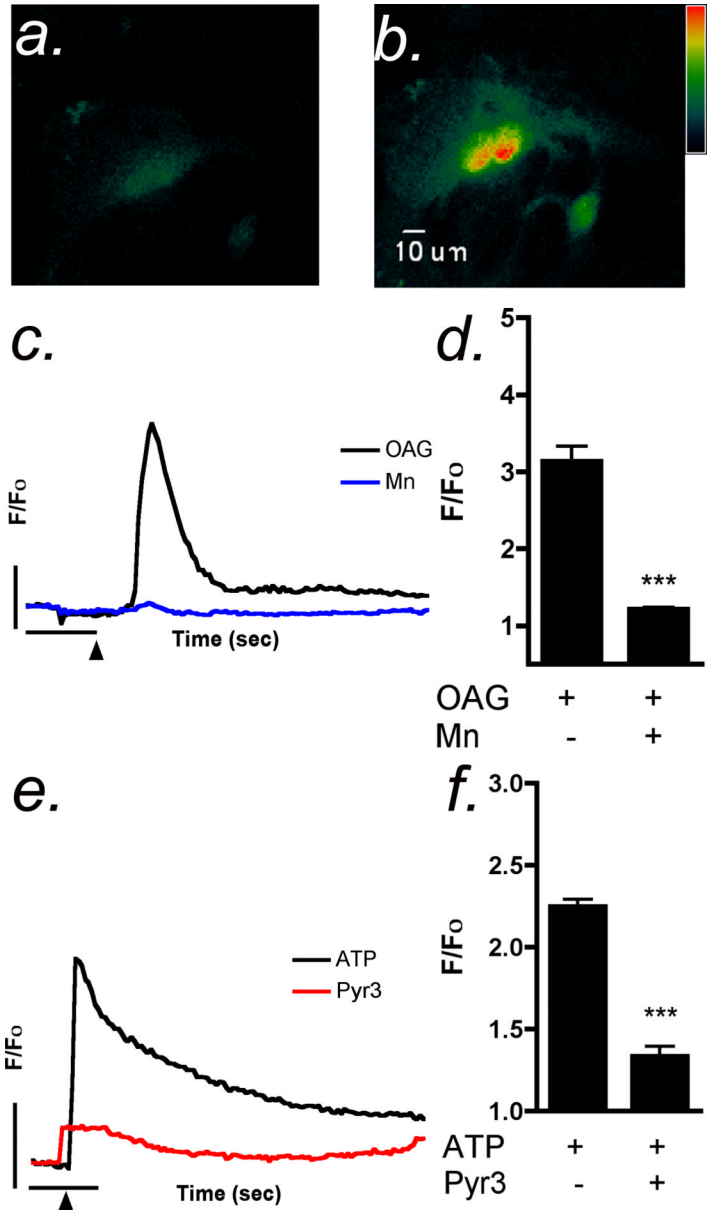

Figure 3. OAG-dependent calcium influx in striatal astrocytes is suppressed by Mn^{2+}

(a,b) Stimulation of striatal astrocytes with the membrane permeable DAG analog, OAG (100 μM), resulted in a robust Ca^{2+} transient in striatal astrocytes, indicated by increases in Fluo-4 fluorescence intensity. (c) Representative traces of OAG-induced intracellular Ca^{2+} transients in the absence (control) and presence of 10 μM Mn^{2+}. (d) Quantitative analysis indicates that the acute application of Mn^{2+} attenuates the OAG Ca^{2+} response in striatal astrocytes. (e,f) The TRPC3 inhibitor, pyrazole-3 (Pyr3) reduces both the peak amplitude and plateau phase of ATP-induced Ca^{2+} transients in striatal astrocytes. Vertical bars denote 1 relative fluorescent unit; horizontal bars denote 10 sec (n=250-400 cells per group; *** p-<0.001).

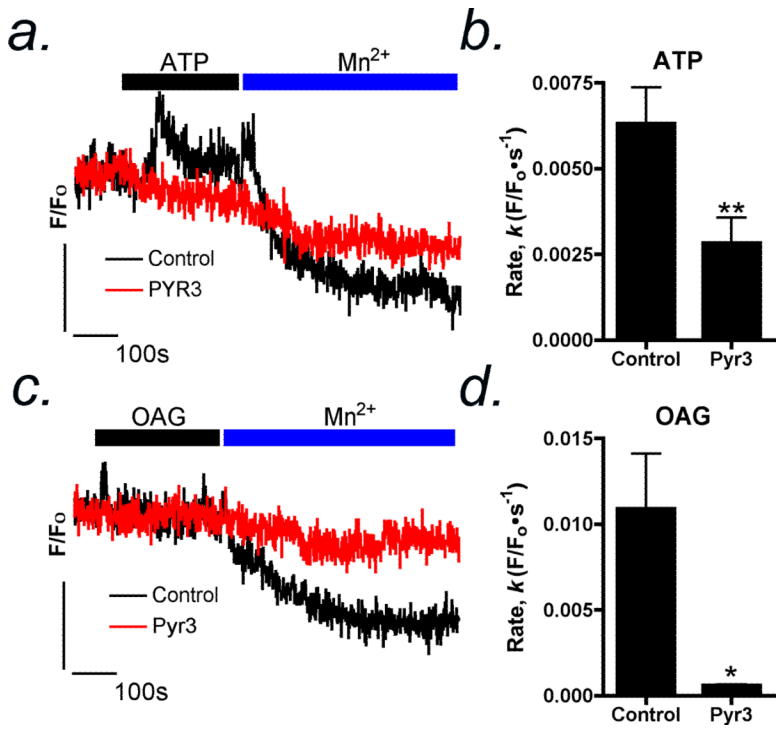

Figure 4. Selective inhibition of TRPC3 reduces the rate of Mn^{2+}-dependent Fura-2 quenching in striatal astrocytes

(a) Following stimulation with 1 μM ATP, Mn^{2+} (100 μM) is rapidly taken up by striatal astrocytes, indicated by quenching of Fura-2 fluorescence intensity. (b) Mn-dependent quenching of Fura-2 fluorescence following ATP stimulation is prevented by the TRPC3 inhibitor, Pyr3. (c) 100 μM OAG induces direct influx of Mn^{2+} from the extracellular medium. (d) Pyr3 inhibits OAG-dependent Mn^{2+} influx and quenching of Fura-2 fluorescence. Data are presented as mean rate of decay of the Fura-2 signal ± SEM. Vertical bars denote 1 relative fluorescent unit; horizontal bars denote 10 sec (n=20-30 cells per group; * p<0.05, ** p<0.01).